An Anti-Lock Braking Control System for a Hybrid Electromagnetic/Electrohydraulic Brake-By-Wire System

Sohel Anwar, *Member, IEEE*

Abstract – **This paper presents a nonlinear sliding mode type controller for slip regulation in a braking event for a hybrid electromagnetic-electrohydraulic brake-by-wire system. The ABS controller modifies the brake torque command generated by a supervisory controller based on driver's command via brake pedal sensor. The brake torque command is then generated by closed loop actuator control algorithms to control the eddy current brake (ECB) and electrohydraulic brake (EHB) systems. The proposed control algorithm shows very good slip regulation in a braking event on low friction coefficient surfaces when compared with non-ABS braking. Usage of ECB resulted in a smooth ABS stop minimizing the NVH of current hydraulic ABS systems.**

I. INTRODUCTION

Anti-locking brake systems (ABS) are well established in the automotive industry as a safety feature. ABS generally offers superior vehicle safety by limiting the longitudinal wheel slip in a braking event with deep slip condition. Drivers would have better directional control of the vehicle equipped with ABS. Most of the ABS systems in the published literature utilize the wheel slip estimate to control the wheel cylinder pressure through a set of valves and a pump in order to regulate the wheel braking torque. These control systems are built around the actuators' dynamic characteristics. With new generation of actuators on the horizon (e.g. electromagnetic, electromechanical, etc.), it may be necessary to design a supervisory vehicle control system that would issue torque command as control input based on vehicle dynamics. The subsystem controller would then close the loop on the actuators based on actuator dynamics. Watanabe et al [13] presented an ABS algorithm that used a vehicle deceleration threshold to activate the brake pressure reduction algorithm and the duration of the pressure pulse was determined by the road friction coefficient. Tan and Chin [12] discussed an ABS algorithm based on sliding mode control theory. Based on a longitudinal one-wheel vehicle model, sufficient conditions for applying sliding mode control to vehicle traction were derived via Lyapunov stability theory. Athan and Papalambros [3] presented a multi-criteria quasi-Monte Carlo method to optimize and compare three ABS nonlinear control algorithms. An adaptive fuzzy logic controller for an anti-lock braking system was discussed by Kokes and Singh [9]. Their controller initially employed a priori training data to control the braking system, but continued to train on-line while continuously updating confidence parameters and placement of fuzzy sets by employing optimization algorithms. Suh et al [11] presented a real time simulator for an anti-lock brake system based on methodology of hardware-in-the-loop simulation using a personal computer. They also provided an analysis and validation of the control logic that used commercial hardware. A genetic algorithm based fuzzy logic controller for ABS systems was the subject of the paper written by Chen and Liao [4]. The controller was based on a nonlinear feedback linearization scheme and fuzzy logic strategy. Given the desired wheel slip-ratio, the feedback linearizing controller cancels all nonlinear dynamics and imposes an appropriate linear behavior on the wheel slip-ratio. Huang and Wang [6] discussed a mixed fuzzy controller to navigate escaping motions of wheeled vehicles under the assumption of Coulomb's viscous friction. The paper focused on modeling, analysis, and control issues of anti-lock braking systems under the assumption of Coulomb's viscous friction while applying the mixed fuzzy controller. Lee and Park [10] presented an ABS algorithm based on sliding mode control in the context of eddy current brakes. However, they consider ABS functionality only at very high speed when the eddy current machine torque is high. Another aspect of this paper is that only a switching function has been used in the paper which tends to cause chatter in the control command. Due to speed dependent torque characteristics of the eddy current machines, the wheels do not fully lock up. This aspect has not been addressed in this paper either.

In the present paper, we present a sliding mode type supervisory ABS control algorithm for a hybrid electromagnetic-electrohydraulic brake-by-wire system for automotive applications. This is a full scale braking system for all speed ranges where the electro-hydraulic brakes compensates for the torque shortfall by the eddy current brakes at lower speed ranges in a smooth fashion. The actuator control algorithm [1] maximizes the eddy current brakes usage keeping the electro-hydraulic friction brake usage to a minimum. The sliding mode type control algorithm uses a saturation function instead of a sign function to minimize chatter in the control command [5]. The resulting ABS system has been verified in a winter test facility with very good results.

Manuscript received September 21, 2003. This work was supported internally by Chassis Advanced Technology Dept. of Visteon Corporation.

S. Anwar is with the Chassis Advanced Technology Dept. of Visteon Corporation, Dearborn, MI 48126 USA (Phone: 313-755-5936; Fax: 313-755-4229; e-mail: sanwar@visteon.com).

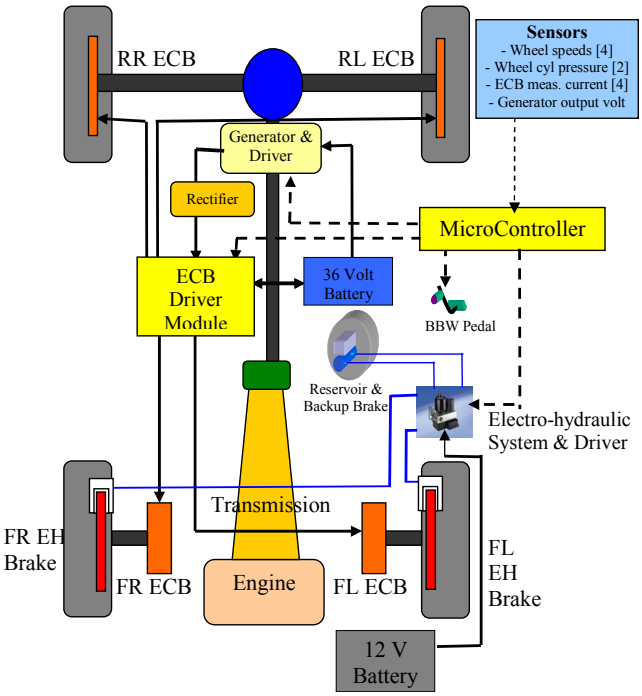

Figure 1 Four wheel ECBs and Electrohydraulic hybrid braking system for a rear wheel drive vehicle.

II. HYBRID BRAKE-BY-WIRE SYSTEM ARCHITECTURE

The BBW configuration (Figure 1) is developed for a rear wheel drive vehicle. It shows that two of the four ECBs are mounted in the rear wheel hubs. The other two are mounted on the sprung mass of the chassis frame and connected to the front wheels via half-shafts. The generator is mounted on the pinion of the rear differential. The BBW pedal assembly replaces the regular brake pedal. Four wheel-speed sensors are mounted on the wheels. Four pressure transducers are used to monitor pressure for the front wheel cylinders and lines. The control algorithm is implemented through a prototype microprocessor based controller (dSPACE). The controller output signals are sent to a power electronics module which channels the electrical power from the generator or the batteries to the appropriate actuators. A 36V battery is used to store the regenerative power and to energize the generator field and occasionally the eddy current brakes depending on system status.

III. MODELING OF THE WHEEL SLIP DYNAMICS

Anti-Lock Brake Systems (ABS) have been around in the cars and trucks for many years. The effectiveness of these systems varies widely depending on the system design, road conditions and driver's response. Most of these systems are based on empirical data and are heavily dependent on testing. In this paper, a more systematic approach is taken to develop an ABS system based on a simplified vehicle model and a sliding mode type control algorithm.

Like most of the ABS control algorithms, the proposed controller also requires the knowledge of wheel slip. The objective of the controller is to keep the wheel slip at a value that would maximize the tire-ground adhesion (or minimize the wheel slip). The wheel slip ratio is obtained from the following definition:

$$\kappa_i(t) = \frac{V_x - R\omega_i}{V_x} \qquad (1)$$

It is necessary to obtain the dynamic equations for the vehicle motion in order to develop the control algorithm. A simplified vehicle model is obtained for a straight line braking event. The vehicle motion in the longitudinal direction on the road plane is described by the following equation [5].

$$\sum F_x = F_{xsum} + F_{tx} - F_{ax} = M(\dot{V}_x - V_y r) + m_s \dot{Z}_s q$$

The wheel rotational dynamics is given by the following equation (Figure 2)

$$\sum M_{yi} = T_{bi} - F_{xi}R + F_{rri}R - T_{di} = -I_{wi}\dot{\omega}_i$$

For a braking event, the following set of equations of motion are written

$$\sum (F_{rri} - F_{xi}) + F_{tx} - F_{ax} = M(\dot{V}_x - V_y r) + m_s \dot{Z}_s q$$

$$T_{bi} - F_{xi}R + F_{rri}R - T_{di} = -I_{wi}\dot{\omega}_i \qquad (2)$$

The pitch dynamics of the vehicle in the first equation is assumed to have negligible effect on the wheel braking forces. For the sake of simplicity, the effect of terrain forces arising out of road slopes and grades are also neglected. The drive torque (in a braking situation) is assumed to be insignificant in the second equation. Further simplification is made by assuming that the steer wheel angle is zero resulting in zero lateral motion. Now, the following relationships are defined:

$$F_{xi} = \mu_i(\kappa)F_{zi};\ F_{rri} = \eta F_{zi}$$

where, $\mu_i(\kappa)$ = Friction Coefficient and η_i =Rolling Resistance Coefficient.

Since a simple model is desired for the proposed controller development, the effect of aerodynamic drag and rolling resistance on the above equation are also neglected. The above assumption is justified based on the fact that the rolling resistance is insignificant compared to the braking force in a braking event. Also, the aerodynamic drag is small for the normal driving speeds. Since this controller is a closed loop system, these effects can be compensated through the feedback information. It is also assumed that the rolling resistance force F_{rri} is much smaller than the friction force F_{xi} and hence neglected.

Thus, equation (2) becomes

$$F_{xsumr} = -\sum \mu_i(\kappa_i)F_{zi}$$

The simplified equations of motion are then given by

$$-\sum \mu_i(\kappa_i)F_{zi} = M\dot{V}_x$$

$$T_{bi} - \mu_i(\kappa_i) F_{zi} R = -I_{wi}\dot{\omega}_i$$

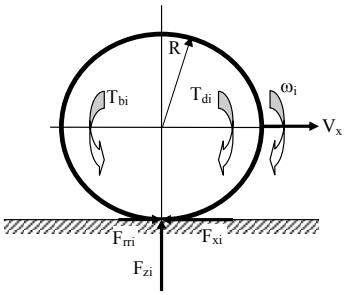

Figure 2 Wheel dynamics in a braking event.

The above set of equations represent plant model for a straight-line braking event. The following section describes the controller development process.

IV. SLIDING MODE TYPE ABS CONTROLLER

Based on the above equations, the plant model for designing a controller is obtained as follows

$$\dot{V}_x = -\frac{1}{M}\sum \mu_i(\kappa_i) F_{zi}$$
$$\dot{\omega}_i = \frac{1}{I_{wi}}\left(-T_{bi} + \mu_i(\kappa_i) F_{zi} R\right) \quad (3)$$

$$\text{Now, } \kappa_i(t) = \frac{V_x - R\omega_i}{V_x} = 1 - \frac{R\omega_i}{V_x}$$

Then, differentiating the above equation yields the following

$$\dot{\kappa}_i = \left(-\frac{R\dot{\omega}_i}{V_x} + \frac{R\omega_i R\dot{V}_x}{V_x^2}\right)$$
$$= -\frac{R}{V_x}\left[\mu(\kappa_i) F_{zi}\frac{R}{I_{wi}} - \frac{1}{I_{wi}} T_{bi}\right] - \frac{R\omega_i}{V_x^2}\frac{1}{M}\sum \mu_i(\kappa_i) F_{zi} \quad (4)$$
$$= \frac{R}{I_{wi}}\frac{1}{V_x} T_{bi} - \frac{R^2}{I_{wi}}\frac{1}{V_x}\mu(\kappa_i) F_{zi} - \frac{R\omega_i}{V_x^2}\frac{1}{M}\sum \mu_i(\kappa_i) F_{zi}$$

Figure 3 shows the friction coefficient curves for a number of tire-ground interfaces. It is evident that the peak of the friction coefficient curve varies significantly depending on the road conditions. The slip ratio value at the peak friction coefficient also varies between 0.1 and 0.2. It is clear that the friction coefficient relationship with slip adds nonlinearity to equation (4). Since all of the curves in figure 3 exhibit approximate linear relationship with slip ratio below the peak of the curve, this relationship between the coefficient of friction and the slip can be approximated with a piecewise linear function. This concept is illustrated in figure 4 [4]. The friction curves are approximated by a straight line with a slope of α_{si} and a slip threshold of κ_{th}. While the peak of these friction curves varies over a slip range, a slip ratio threshold and initial slope can be established for sub-optimal performance.

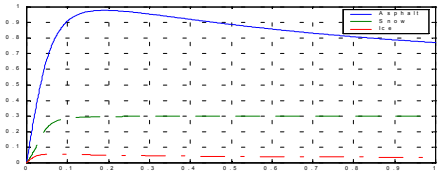

Figure 3 Friction Coefficient vs. Slip Ratio for different surfaces.

An adaptive algorithm can be developed to vary α_{si} in order to represent the actual tire-ground interface relationship to provide optimal braking performance. The piecewise linear friction coefficient-slip ratio relationship can be described as follows:

$$\mu_i(\kappa_i) = \alpha_{si}\kappa_i \qquad if \quad \kappa_i \le \kappa_{th}$$
$$= \alpha_{si}\kappa_{th} \qquad if \quad \kappa_i \ge \kappa_{th} \quad (5)$$

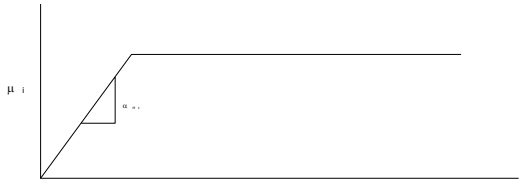

Figure 4 Simplified Friction Coefficient vs. Slip Ratio Curve.

Therefore, equation (4) can be rewritten as

$$\dot{\kappa}_i = \frac{R}{I_{wi}}\frac{1}{V_x} T_{bi} - \frac{R^2}{I_{wi}}\frac{1}{V_x}\alpha_{si}\kappa_i F_{zi} - \frac{R\omega_i}{V_x^2}\frac{1}{M}\sum \alpha_{si}\kappa_i F_{zi} \quad (6)$$

Now, let us define the sliding surface as follows

$$S = (\kappa_{th} - \kappa_i) \quad (7)$$

It is assumed here that the desired slip ratio is same as the slip ratio threshold. With the above definition of the sliding surface, the sliding mode type control law is given by [2],

$$\dot{S} = -\eta SAT\left(\frac{S}{\phi}\right)$$

η = *Convergence Factor*; ϕ = *Boundary Layer Thickness*

Further simplifying,

$$\dot{S} = \dot{\kappa}_{th} - \dot{\kappa}_i = \dot{\kappa}_{th} - \left[\frac{R}{I_{wi}}\frac{1}{V_x} T_{bi} - \frac{R^2}{I_{wi}}\frac{1}{V_x}\alpha_{si}\kappa_i F_{zi} - \frac{R\omega_i}{V_x^2}\frac{1}{M}\sum \alpha_{si}\kappa_i F_{zi}\right] \quad (8)$$

$$\dot{\kappa}_{th} - \frac{R}{I_{wi}}\frac{1}{V_x} T_{bi} + \frac{R^2}{I_{wi}}\frac{1}{V_x}\alpha_{si}\kappa_i F_{zi} + \frac{R\omega_i}{V_x^2}\frac{1}{M}\sum \alpha_{si}\kappa_i F_{zi}$$

Hence, the control law is given by:

$$T_{bi} = \frac{V_x I_{wi}}{R}\dot{\kappa}_{th} + R\alpha_{si}\kappa_i F_{zi} + \frac{I_{wi}}{V_x}\frac{\omega_i}{M}\sum \alpha_{si}\kappa_i F_{zi} + \eta\frac{I_{wi}}{R} V_x * SAT\left(\frac{\kappa_{th} - \kappa_i}{\phi}\right) \quad (9)$$

If κ_{th} is a constant, then the above control law becomes

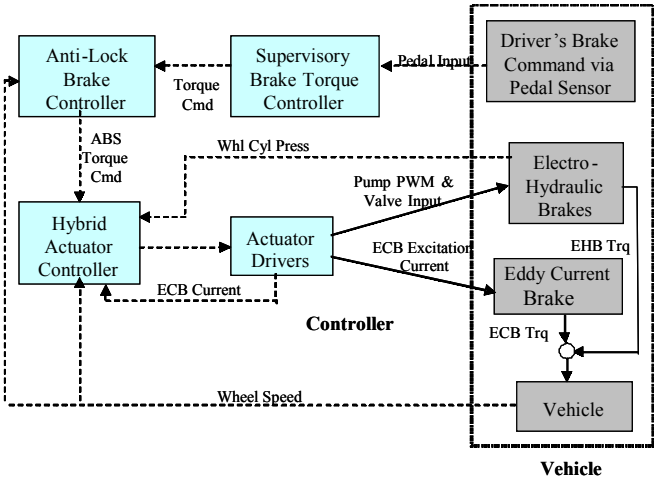

Figure 5 Block diagram representation of the proposed ABS control system.

$$T_{bi} = R\alpha_{si}\kappa_i F_{zi} + \frac{I_{wi}}{V_x}\frac{\omega_i}{M}\sum \alpha_{si}\kappa_i F_{zi} + \eta\frac{I_{wi}}{R}V_x * SAT(\frac{\kappa_{th} - \kappa_i}{\phi}) \quad (10)$$

Equation (10) is the proposed control law for the anti-lock brake control system.

V. CONTROLLER IMPLEMENTATION FOR THE HYBRID ACTUATION SYSTEM

The ABS brake torque command in equation (10) should be applied to the brake actuators at each wheel via a blending algorithm described in section 6. The front wheels have two actuators per wheel: i) eddy current brakes; ii) electrohydraulic friction brakes. The actuator controller tries to maximize the ECB usage while providing the requested torque via EHB in the event the requested brake torque is greater than the estimated available ECB torque. The estimated ECB torque can be calculated using the following equation [3].

$$T(t) = f_0(\omega) + f_1(\omega)i + f_2(\omega)i^2 \quad (11)$$

Where,

T = Retarding torque

i = Retarder feedback current

$$f_0(\omega) = a_{00} + a_{01}\omega + a_{02}\omega^2$$
$$f_1(\omega) = a_{10} + a_{11}\omega + a_{12}\omega^2 \quad (12)$$
$$f_2(\omega) = a_{20} + a_{21}\omega + a_{22}\omega^2$$

a_{00}, a_{01}, … a_{22} = Identified eddy current brake parameters, and ω = Wheel speed.

Figure 5 shows the block diagram representation of the vehicle braking control system. As illustrated, the proposed ABS algorithm works on the desired brake torque command computed by the supervisory brake torque controller. The supervisory brake torque controller receives driver's brake request via pedal sensor (displacement) and interprets the request in terms of desired vehicle deceleration. The desired vehicle deceleration is then utilized to compute desired wheel braking torque based on dynamic front to rear and side-to-side weight transfer.

The ABS controller receives the wheel speed information via wheel speed sensors. The vehicle speed is estimated via a proprietary estimation algorithm. The wheel slip ratio is then calculated based on measured wheel speed and estimated vehicle speed. The normal force on each wheel is estimated via static load distribution. The slope of the friction-coefficient vs. slip ratio curve is either known or estimated. The experimental data presented in section VI is based on a known value of the friction coefficient. The vehicle parameters such as vehicle mass, wheel inertia, and wheel rolling radius are computed based on direct measurements. With this information, the ABS torque command can now be computed using equation (10). Once the actuator controller receives the torque command from the ABS controller, it estimates the maximum available torque for the eddy current brakes at a given wheel speed. If the ABS torque command is larger than the eddy current brake available torque, then the eddy current brake is commanded full excitation current via 100 percent PWM duty cycle to the ECB driver. The difference between the requested torque and the estimated ECB torque is then translated into desired wheel cylinder pressure for the EHB. The actuator controller regulates the desired ECB current and desired EHB pressure in a closed loop fashion via current and pressure feedback.

VI. EXPERIMENTAL RESULTS

The proposed ABS control system was implemented on a Brake-By-Wire (BBW) vehicle previously developed. The BBW vehicle has hybrid actuators for the front wheels and only ECBs on the rear wheels. Since the eddy current brakes have speed dependent torque characteristics, the rear wheels did not have any significant slip. A Chevrolet Silverado was used as the test vehicle. The front eddy current brakes are mounted on the sprung mass of the vehicle and are connected to the wheels via half-shafts. The vehicle was instrumented with a number of instrument grade sensors. Wheel speeds and torques are measured using Michigan Scientific sensors. Vehicle longitudinal acceleration is measured via Texas Instrument capacitive accelerometer. The current sensors were made in house with off-the-shelf components and were integrated with the ECB driver modules.

Tests were performed for straight line braking on packed snow. These tests were run with and without the ABS controller activated. The horizontal axis for all the plots in Figures 6 through 15 represent time in seconds. Figure 6

shows the wheel speeds for all four wheels in a straight line braking event on packed snow without the proposed ABS controller activated. It shows that front wheels quickly lock up due to excessive hydraulic pressure at the wheel cylinder which is direct result of driver's request. Figure 7 shows the wheel speeds for the vehicle in a braking event on packed snow surface, with the proposed ABS algorithm activated. The desired slip ratio for packed snow surface was set at 0.2 where the friction coefficient is at its maximum. The front wheels did not lock up, instead they maintained a slip ratio close to desired value as observed from the difference between front wheel speeds and non-skidding rear wheel speeds.

Figure 8 illustrates the slip ratio for the straight line braking event on packed snow without ABS activated. As the front wheels locked up, the slip ratio for the front wheel reached a value of unity, indicating 100 percent skidding (or full lock up). Figure 9 shows the slip ratio for the straight line braking on packed snow, but with the proposed ABS algorithm activated. As illustrated, the front wheel slip ratio is maintained at around the desired slip ratio value of 0.2 or 20 percent slip.

Figure 10 and Figure 11 show the commanded wheel braking torque from the supervisory brake-by-wire controller for non-ABS and ABS activated controls respectively. Clearly, the commanded torques reached the maximum values quickly after brake is applied in a non-ABS case. However, for ABS activated condition, the command torque is modified by the ABS control law and is modulated to keep the wheel slip ratio near the desired value.

Figures 12 and 13 show the measured wheel torque values for all four wheels in non-ABS and ABS conditions respectively. For the front wheels, the electrohydraulic friction brakes cause the wheel to lock up very quickly as illustrated in Figure 6. In the ABS mode, however, the measured torque is reduced to a level to maintain the desired slip ratio at each of the front wheels.

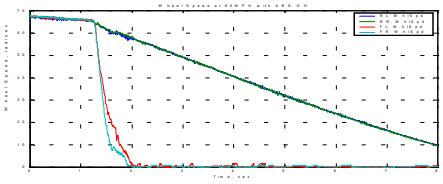

Figure 6 Wheel speeds (rad/s) for the vehicle on packed snow surface without ABS activated.

Figures 14 and 15 show the measured excitation current to the eddy current brakes for non-ABS and ABS activated cases respectively. As illustrated in Figure 14, the excitation currents to the front eddy current brakes drop quickly to zero as the wheels get locked up by the friction brakes. In the ABS activated case, the excitation currents to the front wheel eddy current brakes are only minimally modulated based on the ABS torque command and torque producing capability of the ECBs. Most of the torque reduction in the wheel braking torque command occurs in the electrohydraulic brake command, resulting in maximum usage of the eddy current brake.

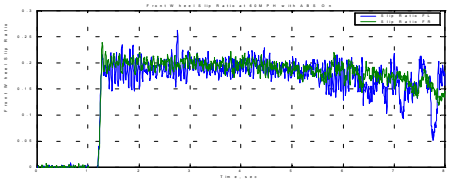

Figure 7 Wheel slip ratio for the vehicle on packed snow surface with ABS activated.

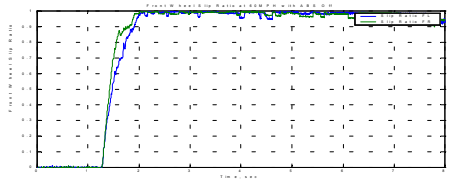

Figure 8 Wheel slip ratio for the vehicle on packed snow surface without ABS activated.

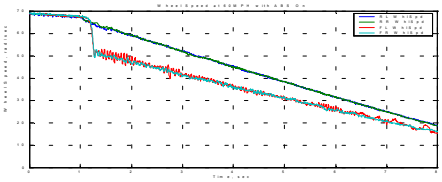

Figure 9 Wheel speeds (rad/s) for the vehicle on packed snow surface with ABS activated.

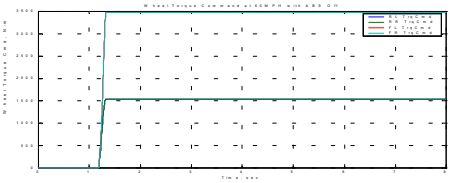

Figure 10 Wheel brake torque command (N-m) for the vehicle on packed snow surface without ABS activated.

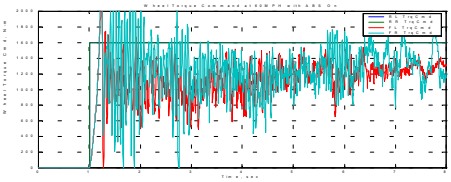

Figure 11 Wheel torque command (N-m) for the vehicle on packed snow surface with ABS activated.

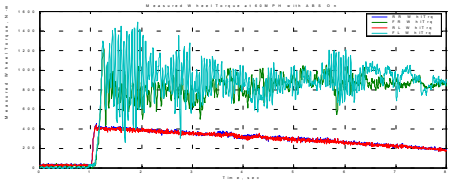

Figure 12 Measured wheel torque (N-m) for the vehicle on packed snow surface without ABS activated.

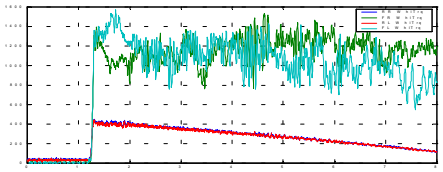

Figure 13 Measured wheel torque (N-m) for the vehicle on packed snow surface with ABS activated.

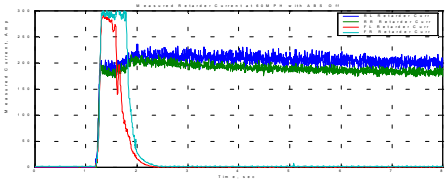

Figure 14 Measured current to wheel-end eddy current brakes for the vehicle on packed snow surface without ABS activated.

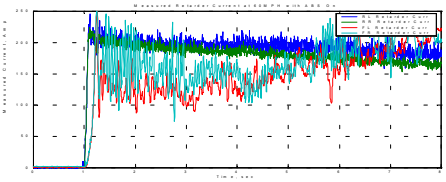

Figure 15 Measured current to wheel-end eddy current brakes for the vehicle on packed snow surface with ABS activated

VII. CONCLUSIONS

A nonlinear sliding mode type controller is presented for slip regulation in a braking event for a hybrid electromagnetic-electrohydraulic brake-by-wire system. Experimental results show very good slip regulation in braking event on a low friction coefficient surface when compared with non-ABS braking condition. It has been observed that the eddy current brakes provided most of the torque while the electrohydraulic brake compensated for the difference between ABS torque command and estimated eddy current brake torque. The result is a very smooth ABS stop, thus minimizing the NVH (noise, vibration, and harshness) of current hydraulic ABS systems. The vehicle steerability could be fully maintained while changing a lane on a low friction coefficient surface with the ABS algorithm presented in this paper.

VIII. NOMENCLATURE

V_x = Vehicle longitudinal speed in road co-ordinate system
F_{xsum} = sum of road forces in the x-direction; F_{tx} = Terrain forces at the c.g.; F_{ax} = Aerodynamic drag forces
M = Total vehicle mass; m_s = Sprung mass of the vehicle
R = Wheel Rolling radius; I_{wi} = i-th wheel rotational inertia
$\dot{V}_x$ = Vehicle longitudinal acceleration; $\omega_i, \dot{\omega}_i$ = Angular speed and acceleration of the i-th wheel
V_y = Vehicle lateral velocity; r = Vehicle yaw velocity
q = Pitch velocity of the sprung mass; $\dot{Z}_s$ = Sprung mass velocity in the Z-direction
T_{bi} = Brake torque at the i-th wheel; T_{di} = Drive torque at the i-th wheel ; F_{xi} = Longitudinal friction force at the i-th tire; F_{rri} = Rolling Resistance at the i-th tire;

IX. REFERENCES

[1] S. Anwar and B. Ashrafi., "Development of a Hybrid Electromagnetic/Electrohydraulic Brake-By-Wire System at Visteon", Technical Report No. B600-027, Chassis Advanced Technology, Visteon Corporation, May 2003.

[2] S. Anwar, "A Parametric Model of an Eddy Current Electric Machine for Automotive Braking Applications", to appear in *IEEE Transactions on Control Systems Technology,* November, 2003.

[3] T. W.Athan and P. Y. Papalambros, "Multicriteria Optimization of Anti-Lock Braking System Control Algorithms", Engineering Optimization, Vol. 27, No. 3, pp. 199-227, 1996.

[4] F. W. Chen and T. L. Liao, "Nonlinear Linearization Controller and Genetic Algorithm-Based Fuzzy Logic Controller for ABS Systems and Their Comparison", International J. of Vehicle Design, Vol. 24, No. 4, pp. 334-349, 2000.

[5] J. K. Hedrick, "Analysis and Control of Nonlinear Systems", Journal of Dynamics Systems, Measurement, and Control, Vol. 115, June, 1993.

[6] H-P. Huang. and C-K. Wang., "Intelligent Control of Wheeled Vehicles with Anti-Braking Systems", International Journal of Vehicle Design, Vol. 26, No. 2-3, pp. 218-238, 2001.

[7] S. Kimbrough, "Brake Control Algorithms", Final Report, Mechanical Engineering Dept., University of Utah, 1997.

[8] U. Kiencke and L. Nielsen, "Automotive Control System for Engine, Driveline, and Vehicle", SAE International, 2000.

[9] G. Kokes and T. Singh., "Adaptive Fuzzy Logic Control of an Anti-Lock Braking System", IEEE Conference on Control Applications – Proceedings, Vol. 1, pp. 646-651, 1999.

[10] K. Lee and K. Park, " Optimal Robust Control of a Contactless Brake System using an Eddy Current", Mechatronics, Vol. 9, No. 6, pp. 615, 1999.

[11] M.W. Suh, J.H. Chung, C.S. Seok, and Y.J. Kim, "Hardware-in-the-Loop Simulation for ABS based on PC", International Journal of Vehicle Design, Vol. 24, No. 2, pp. 157-170, 2000.

[12] H-S. Tan and Y-K. Chin, "Vehicle Traction Control. Variable-Structure Control Approach", J. Dynamic System, Measurement, & Control, Trans. of the ASME, Vol. 113, No. 2, pp. 23-230, 1991.

[13] M. Watanabe and N. Noguchi, "New Algorithm for ABS to compensate for Road Disturbances", SAE Transactions, Vol. 99, No. Sec. 6, pp. 271-279, 1990.